

Construction of Two-Faced (Hetero)hydrocarbyl Diiron Complexes Mediated by the Interplay of Ligands

Chiara Zappelli, Gianluca Ciancaleoni,* Stefano Zacchini, and Fabio Marchetti*



Cite This: *Organometallics* 2023, 42, 615–626



Read Online

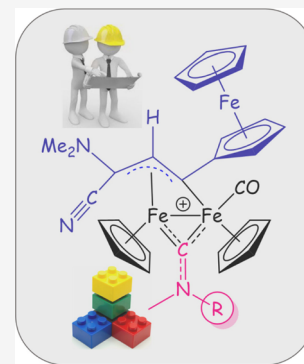
ACCESS |

Metrics & More

Article Recommendations

Supporting Information

ABSTRACT: The functionalized allylidene complex $[\text{Fe}_2\text{Cp}_2(\text{CO})(\mu\text{-CO})\{\mu\text{-}\eta^1\text{:}\eta^3\text{-C}^\alpha(\text{Fc})\text{-C}^\beta\text{HC}^\alpha(\text{CN})\text{NMe}_2\}]$, **1** [$\text{Cp} = \eta^5\text{-C}_5\text{H}_5$; $\text{Fc} = \text{CpFe}(\eta^5\text{-C}_5\text{H}_4)$], reacted with isocyanides (CNR), in isopropanol solution at ca. 100 °C, to give the CO-substitution products $[\text{Fe}_2\text{Cp}_2(\text{CO})(\mu\text{-CNR})\{\mu\text{-}\eta^1\text{:}\eta^3\text{-C}^\alpha(\text{Fc})\text{-C}^\beta\text{HC}^\alpha(\text{CN})\text{NMe}_2\}]$ [$\text{R} = \text{CH}_2\text{P}(\text{O})(\text{OEt})_2$, **2a**; $\text{R} = 2\text{-naphthyl}$, **2b**; $\text{R} = \text{CH}_2\text{C}(\text{O})(\text{OEt})$, **2c**], which were isolated in 61–84% yields. The bridging coordination of CNR in **2a–c** is forced by a stabilizing electrostatic interaction between the nitrogen lone pair belonging to the $\{\text{NMe}_2\}$ group and the terminal CO ligand. Isocyanide methylation with methyl triflate proceeded with the inversion of stereochemistry at the C^α carbon and led to $[\text{Fe}_2\text{Cp}_2(\text{CO})\{\mu\text{-CN}(\text{Me})\text{R}\}\{\mu\text{-}\eta^1\text{:}\eta^3\text{-C}^\alpha(\text{Fc})\text{-C}^\beta\text{HC}^\alpha(\text{CN})\text{NMe}_2\}]\text{CF}_3\text{SO}_3$ ($\text{R} = \text{CH}_2\text{P}(\text{O})(\text{OEt})_2$), (**[3a]** CF_3SO_3 ; $\text{R} = 2\text{-naphthyl}$, **[3b]** CF_3SO_3), containing bridging allylidene and aminocarbyne ligands (68–74% yields). All products were fully characterized by IR and multinuclear NMR spectroscopy, and the structures of **2a** and **[3a]** CF_3SO_3 were elucidated by X-ray diffraction studies. Density functional theory (DFT) calculations were extensively carried out to shed light on structural, mechanistic, and thermodynamic features.



1. INTRODUCTION

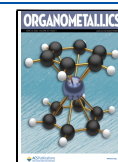
Dimetallic complexes featuring two adjacent metal centers constitute unique systems in coordination chemistry, in that such a dimetallic core is the simplest framework which benefits from cooperative effects, enabling peculiar reactivity patterns (especially on bridging ligands) otherwise not viable on monometallic complexes.^{1–5} Thus, dimetallic complexes have been widely investigated as convenient models to clarify and develop chemical transformations mediated by more complex structures wherein the metal–metal synergy plays a key role, such as natural enzymes and metal surfaces.^{6,7} In this setting, the interest in the reactivity of hydrocarbyl ligands, bridging coordinated in dinuclear metal complexes, ranges from the elucidation of the mechanisms of carbon–carbon bond formation processes (e.g., the Fischer–Tropsch synthesis),^{8–12} the metal-mediated synthesis of organic compounds,^{13,14} new organometallic motifs not accessible from conventional procedures,^{15–18} and the formation of complexes with functionalized ligands supplying useful properties for applications in catalysis, electronics, and medicinal chemistry.^{19–23} The huge and urgent demand for the development of sustainable synthetic methodologies renders diiron complexes an ideal choice to explore novel organometallic reaction pathways based on the abundance and environmental benignity of iron.^{11,24–27}

Our experience with the chemistry of diorganoirron complexes concerns the use of the easy-to-handle and inexpensive $[\text{Fe}_2\text{Cp}_2(\text{CO})_4]$ (Fp_2 , $\text{Cp} = \eta^5\text{-C}_5\text{H}_5$) as a starting material. The stepwise replacement of one or two carbonyl ligands allows the assembly of small organic units affording

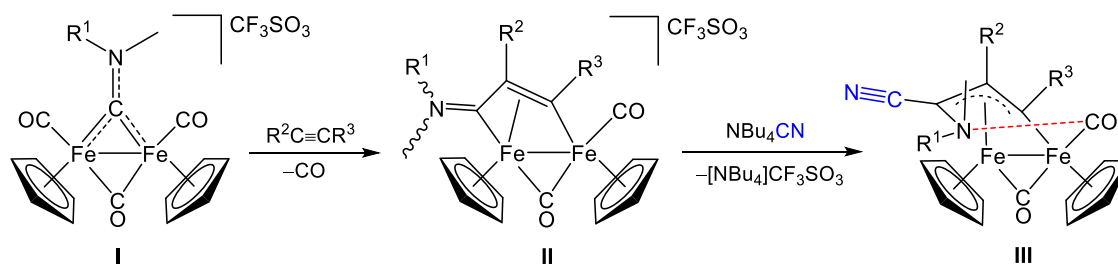
derivatives with a bridging unsaturated CHN ligand (aminocarbyne or vinyliminium; **Scheme 1**), displaying a rich and versatile reactivity that opens the doors to a diversity of structural modifications.^{20,28,29} In particular, diiron vinyliminium complexes (structure **II** in **Scheme 1**) compose a class of potentially unlimited organometallics due to the broad availability of alkynes, $\text{R}^2\text{C}\equiv\text{CR}^3$, employed for their synthesis from aminocarbyne precursors (**I**). A family of allylidene derivatives of **II** is obtained by cyanide addition (**Scheme 1**), which usually occurs at the iminium carbon, unless a sterically demanding group is placed on the nitrogen.^{30,31} Notably, this reaction is general, working with a variety of substituents R^{1-3} , and proceeds in a stereoselective mode, i.e., locating the cyano group in the syn position with respect to the adjacent R^2 . DFT investigation on a complex of type **III** ($\text{R}^1 = \text{Me}$, $\text{R}^2 = \text{H}$, $\text{R}^3 = \text{Ph}$) outlined that the observed stereoselectivity is due to the interaction between the nitrogen lone pair belonging to the amine group and the carbon of the terminal CO ligand (calculated $\text{C}\cdots\text{N}$ distance = 2.425 Å).³¹ In principle, such an interaction provides a stabilization to the overall structure; otherwise, it is expected to weaken the Fe–CO binding, thus potentially favoring the CO replacement by other ligands. Our

Received: February 9, 2023

Published: March 29, 2023

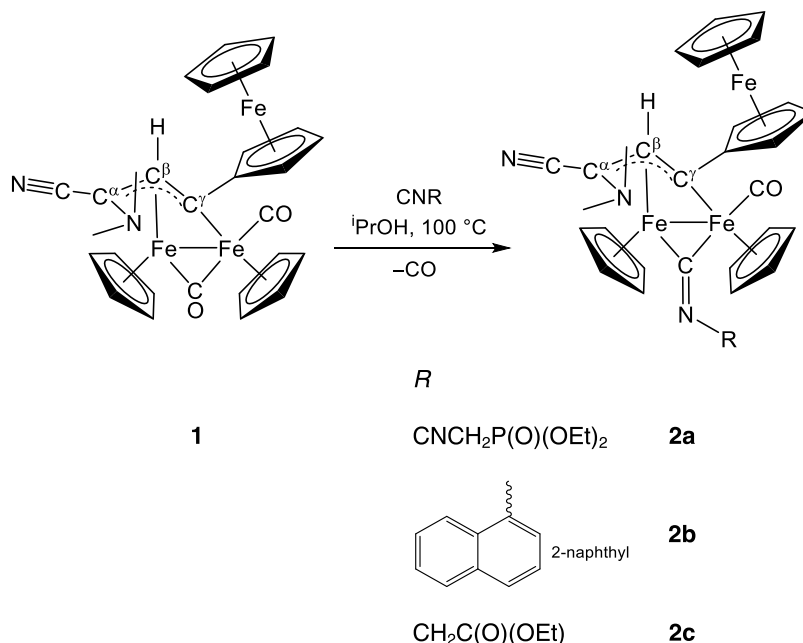


Scheme 1. General Structures of Diiron Complexes Derived from $[\text{Fe}_2\text{Cp}_2(\text{CO})_4]$ Containing a Bridging Aminocarbyne (I) or Vinyliminium (II) Ligands, and Regio- and Stereoselective Cyanide Addition to the Iminium Carbon Affording (Cyano)amino-allylidene Complexes (III)^a



^aRed dashed line: interaction between amine-nitrogen lone pair and carbonyl carbon.

Scheme 2. Installation of Bridging Isocyanide Ligand in Ferrocenyl-Decorated Diiron (Cyano)amino-allylidene Complexes via Thermal CO Replacement



interest was focused on isocyanides, which may be incorporated in organometallic structures by the substitution of CO ligands and are versatile substrates susceptible to further transformations once coordinated to a metal center.^{32–37}

Herein, we report a study on the reactivity of a selected complex of type **III**, showing that the complexity of the system is crucial to finely drive the reaction outcomes, leading to an example of a dimetallic structure comprising two heterofunctionalized hydrocarbyl ligands occupying the two bridging coordination sites.

2. RESULTS AND DISCUSSION

2.1. Carbon Monoxide-Isocyanide Substitution Reaction. We selected for the present study the recently reported ferrocenyl-decorated (cyano)amino-allylidene complex **1**.^{38,39} The reactions of **1** with a series of isocyanides, in isopropanol solution at ca. 100 °C, proceeded with CO-CNR replacement to give the novel compounds **2a–c**, which were isolated after workup in moderate to high yields (Scheme 2).

Products were fully characterized by IR and multinuclear NMR spectroscopy; moreover, the structure of **2a**, containing a bridging diethyl isocyanomethylphosphonate ligand, was

ascertained by X-ray diffraction (Figure 1 and Table 1). The replacement of $\mu\text{-CO}$ by $\mu\text{-CNCH}_2\text{P}(\text{O})(\text{OEt})_2$ in the structure of **2a** does not significantly alter the geometry and bonding parameters of the (cyano)amino-allylidene ligand, compared to the parent compound **1**³⁸ and related complexes lacking the ferrocenyl unit.^{30,31} In particular, both C(2)–C(3) [1.447(14) Å] and C(3)–C(4) [1.418(13) Å] contacts display some π -character, whereas C(2)–N(1) [1.426(12) Å] is essentially a single bond. In agreement with this, N(1) [sum angles 334.4(14)°] shows a considerable pyramidalization, indicative of sp^3 hybridization. A weak sub van der Waals contact is present between N(1) and the terminal carbonyl carbon atom [N(1)⋯C(1) 2.65(2) Å], as also found in **1** [2.71(2) Å]. Previously, $[\text{FePt}(\text{CO})_3(\text{PPh}_3)(\text{dppm})\{\mu\text{-CNCH}_2\text{P}(\text{O})(\text{OEt})_2\}]$ was the only compound structurally characterized containing the same bridging isocyanide ligand, and the bonding parameters of $\mu\text{-CNCH}_2\text{P}(\text{O})(\text{OEt})_2$ are similar to those found in **2a**.⁴⁰ In **2a**, the C(11)–N(2) contact [1.202(13) Å] is rather short, suggesting a relatively scarce π -back-donation from the iron centers to the bridging isocyanide, in comparison with that documented for other diiron $\mu\text{-CNR}$ systems.^{41,42}

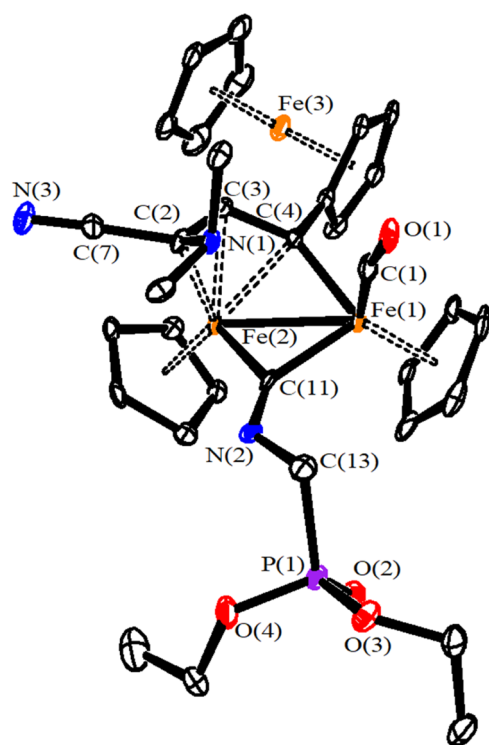


Figure 1. View of the molecular structure of **2a**. Displacement ellipsoids are at the 30% probability level. H atoms have been omitted for clarity.

The structure of **2a** was also DFT-calculated, and six different isomers were optimized (**2aA**–**2aE**; see [Table 2](#) and [Figure S13](#)). The most stable isomer (**2aA**) displays the cis configuration of the Cp rings and the methylphosphonate group pointing to the carbonyl ligand, coherently with the structure of **2a** experimentally detected in the solid state.

In **2aA**, the nitrogen of the NMe₂ group (N^A) points to the carbon of the terminal CO (C^t), with a N^A⋯C^t distance of 2.596 Å (experimental 2.653 Å) (see [Table 1](#)). This interaction can be studied in more detail using the natural bond orbital (NBO) framework and, specifically, the second-order perturbation theory interaction energy analysis ($E^{(2)}$). The latter characterizes the interaction between occupied and unoccupied NBO-typed Lewis orbitals that contribute to the electron delocalization from bonding (BD) or lone pair (LP) orbitals to antibonding orbitals (BD*) or unfilled valence-type nonbonding orbitals (LV). In **2aA**, there is a stabilizing contribution from the donor–acceptor (D–A) pair LP1(N^A) → LV1(C^t), the corresponding $E^{(2)}$ value being 23.1 kcal/mol ([Table 3](#)). A similar contribution exists for the D–A pair LP1(N^A) → BD*1(C^tO), where BD*1(C^tO) is the most stable unoccupied antibonding orbital of the CO moiety ($E^{(2)}$ = 0.9 kcal/mol). These contributions compete with the Fe¹ → CO back-donation, which involves the LP1(Fe¹) → LV1(C^t), $E^{(2)}$ = 27.3 kcal/mol, LP1(Fe¹) → BD*1(C^tO), $E^{(2)}$ = 4.4 kcal/mol, LP2(Fe¹) → LV1(C^t), $E^{(2)}$ = 13.5 kcal/mol, and LP2(Fe¹) → BD*1(C^tO), $E^{(2)}$ = 16.8 kcal/mol, where LP1(Fe¹) and LP2(Fe¹) are two different lone pairs centered on the metal.

On the other hand, the NBO analysis of **2aB**, wherein the Me₂N^A⋯C^tO interaction is hampered by the *trans* arrangement of the Cp ligands, shows that the Fe¹ → C^tO back-donation

components are much larger, especially LP1(Fe¹) → LV2(C^t), whose $E^{(2)}$ results in 64.0 kcal/mol ([Table 3](#)).

In **2aE**, bearing a bridging CO and a terminal CNR ligand, the isocyanide and the amine group can interact in principle, but all parameters indicate that this potential interaction is weak. Indeed, the Me₂N⋯CNR distance is 2.820 Å, sensibly longer than the analogous one in **2aA** (Me₂N⋯CO, 2.596 Å). The corresponding NBO D → A pair (LP1(N^A) → BD*2(CN)) has an $E^{(2)}$ of only 3.3 kcal/mol, whereas in **2aA** the pairs involving the amine and the terminal CO have a total value of $E^{(2)}$ of 24 kcal/mol. The relatively weak amine⋯terminal CNR interaction, compared to amine⋯terminal CO, accounts for the lower stability of **2aE** with respect to **2aA**.

The spectroscopic data related to **2a**–**c** in organic solvents are fully consistent with the solid-state structure ascertained for **2a** ([Table S1](#)). The IR spectra, recorded in the 2300–1500 cm⁻¹ range (CH₂Cl₂ solutions), share a common pattern consisting of three bands, attributed to the cyano moiety (ca. 2190 cm⁻¹), the terminal carbonyl ligand (ca. 1960 cm⁻¹), and the bridging isocyanide ligand (ca. 1705 cm⁻¹). Thus, infrared data clearly indicate that the carbonyl-isocyanide substitution reaction proceeds with the selective occupation of the bridging coordination site by CNR and confirm the presence of the relatively strong isocyanide C–N bond (see the discussion of the X-ray structure of **2a**). For sake of comparison, the stretching vibration related to the bridging isocyanomethylphosphonate ligand falls at 1705 cm⁻¹ in **2a** and at 1648 cm⁻¹ in the iron-platinum complex [FePt(CO)₃(PPh₃)(dppm){μ-CNCH₂P(O)(OEt)₂}]⁴⁰. The carboxylato group in **2c** gives rise to an absorption at 1723 cm⁻¹. In the bis-carbonyl precursor **1**, the stretching vibration related to the terminal carbonyl falls at 1967 cm⁻¹;³⁸ therefore, the replacement of μ-CO with μ-CNR on going from **1** to **2a**–**c** determines a slight increase of the Fe → t-CO π-back-donation.

In agreement with the X-ray evidence collected for **2a**, NMR spectra point out that the bridging allylidene ligand in **2a**–**c** is substantially unchanged with respect to the parent compound **1** ([Table S1](#)). In particular, the resonances related to the C^βH unit have been found in the narrow intervals 5.38–5.42 ppm (¹H) and 82.9–83.7 ppm (¹³C), while the corresponding values for **1** are 5.42 and 83.3 ppm, respectively. Similarly, the C^α and C^γ resonances undergo a minor shift on going from **1** to **2a**–**c**, and in **2a**–**c** they occur at 63.5–65.9 and 196.6–197.6 ppm, respectively. The C^γ carbon is almost equidistant between the two iron centers and possesses a bridging alkylidene nature, which is reflected in the low-field ¹³C NMR signal.^{43–46} Likewise in **1**, the N-methyl groups are nonequivalent in **2a**–**c**, confirming the occurrence of intramolecular amine–CO interaction in solution [e.g., for **2a**: δ(¹H) = 2.27, 1.75 ppm; δ(¹³C) = 50.3, 41.5 ppm]. The phosphorus nucleus belonging to the isocyanide substituent in **2a** is considerably affected by coordination, as witnessed by the shift of the related ³¹P NMR resonance (from 14.0 ppm in uncoordinated isocyanide to 24.0 ppm in **2a**).

While the NMR spectra of **2a,c** consist of single sets of resonances, the spectra of **2b** reveal the presence of two isomeric species. We hypothesize that the two isomers are *cis* and *trans* (with reference to the mutual arrangement of the Cp rings with respect to the Fe–Fe axis), the *cis* isomer being largely prevalent in accordance with DFT outcomes (*vide infra*). More precisely, the Cp resonances are found, in the ¹H NMR spectrum, at 4.88 and 4.37 ppm (*cis*) and 4.84 and 4.54 ppm (*trans*). A comparative view of the ¹H NMR data of **2a**–**c**

Table 1. Comparative View of Selected Bond Lengths (Å) and Angles (°) for 1 (Experimental),³⁸ 2a (Experimental and Calculated), and [3a]⁺ (Experimental and Calculated)

	1 (X-ray)	2a (X-ray)	2aA (DFT)	[3a] ⁺ (X-ray)	[3a] ⁺ (DFT)
Fe(1)–Fe(2)	2.5379(6)	2.5380(17)	2.528	2.5324(14)	2.502
Fe(1)–C(1)	1.771(3)	1.777(10)	1.738	1.787(8)	1.736
Fe(2)–C(2)	2.071(3)	2.098(9)	2.109	2.118(7)	2.162
Fe(2)–C(3)	2.025(3)	2.016(10)	1.995	2.037(7)	2.021
Fe(2)–C(4)	2.025(3)	2.007(10)	2.002	2.025(7)	1.998
Fe(1)–C(4)	1.964(3)	1.963(9)	1.963	1.975(6)	1.966
Fe(1)–C(11) ^a	1.922(3)	1.962(11)	1.917	1.899(7)	1.855
Fe(2)–C(11) ^a	1.911(3)	1.927(10)	1.879	1.878(6)	1.847
Fe(1)–Cp _{Ct} ^b	1.747(5)	1.748(5)	1.781	1.760(5)	1.779
Fe(2)–Cp _{Ct} ^b	1.716(5)	1.721(7)	1.724	1.732(2)	1.731
Fe(3)–Cp _{Ct} ^{ab}	1.651(3)	1.654(2)	1.639	1.662(2)	1.642
Fe(3)–Cp _{Ct} ^{bb}	1.653(5)	1.648(2)	1.632	1.654(2)	1.628
C(1)–O(1)	1.142(4)	1.143(12)	1.171	1.131(9)	1.162
C(2)–N(1)	1.447(4)	1.426(12)	1.434	1.447(10)	1.439
C(2)–C(3)	1.446(4)	1.447(14)	1.449	1.423(11)	1.440
C(3)–C(4)	1.414(4)	1.418(13)	1.424	1.424(11)	1.425
C(2)–C(7)	1.467(5)	1.469(13)	1.448	1.476(9)	1.444
C(7)–N(3)	1.145(4)	1.142(13)	1.175	1.136(10)	1.174
C(11)–N(2)		1.202(13)	1.249	1.292(9)	1.315
N(2)–C(12)				1.477(9)	1.477
N(2)–C(13)		1.445(13)	1.436	1.469(10)	1.464
C(13)–P(1)		1.809(11)	1.837	1.821(7)	1.842
P(1)–O(2)		1.468(7)	1.507	1.463(5)	1.506
P(1)–O(3)		1.563(8)	1.638	1.562(7)	1.612
P(1)–O(4)		1.556(8)	1.626	1.574(8)	1.628
Fe(1)–C(1)–O(1)	169.1(3)	167.8(9)	163.17	171.9(9)	172.75
Fe(1)–C(11)–Fe(2)	82.94(13)	81.5(4)	83.49	84.2(3)	85.04
Fe(1)–C(4)–Fe(2)	79.01(11)	79.5(4)	79.18	78.5(2)	78.28
Fe(1)–C(4)–C(3)	125.0(2)	124.5(8)	124.36	123.3(5)	123.85
C(4)–C(3)–C(2)	123.6(3)	123.3(9)	122.93	127.4(6)	128.38
C(3)–C(2)–N(1)	121.2(3)	123.0(8)	120.32	113.8(6)	115.13
Sum at N(1)	334.4(4)	334.4(14)	341.70	335.2(10)	342.55
C(2)–C(7)–N(3)	179.3(4)	176.4(12)	174.60	172.5(10)	169.13
C(11)–N(2)–C(13)		127.4(9)	127.93	122.8(6)	122.26
N(2)–C(13)–P(1)		109.0(7)	110.00	113.2(5)	112.20

^aC(11) is bonded to O in **1** and to N in [2a]⁺ and [3a]⁺. ^bCp_{Ct} is the centroid of the cyclopentadienyl ligand. For Fe(3), Cp^a is the substituted cyclopentadienyl and Cp^b=Cp.

Table 2. Gibbs Free Energies (in kcal/mol) and Descriptors for the Spatial Arrangement of 2a-Related Structures

isomer	ΔG	Cp/Cp	R/CO	CNR
2aA	0.0	cis	cis	bridging
2aB	6.2	trans	cis	bridging
2aC	1.1	cis	trans	bridging
2aD	5.4	trans	trans	bridging
2aE	5.2	cis	cis	terminal
2aF	6.4	trans	trans	terminal

points out that **2a** and **2c** adopt the Cp-cis geometry, according to the X-ray evidence for **2a**.

The structure of **2b** was optimized by DFT calculations, evaluating the relative stability of possible structures (**2bA–F**) (see Table 4 and Figure S14). The most stable isomer (**2bA**) is homologous to **2aA** and thus exhibits a cis geometry of the Cp ligands and the naphthyl group on the same side as the CO ligand. In **2bA** as in **2aA**, the NMe₂ moiety directs the nitrogen lone pair toward the CO carbon (N⋯C distance 2.635 Å, C–

O distance 1.172 Å), and the NBO analysis reveals a weak N⋯C interaction at the expense of the Fe → CO π back-donation.

The substitution reaction affording **2a–c** deserves further comments. It is a common feature in organometallic chemistry that isocyanides replace carbonyl ligands, and thermal treatment is often used as an effective method.^{32,47,48} Nevertheless, here the presence of the bridging unsaturated hydrocarbyl ligand (allylidene) might favor the formation of C–C coupling products,⁴⁹ which, however, have not been observed.

In dinuclear metal systems, mixtures of isomers may be obtained as CO-CNR substitution products, resulting from the competition for bridging coordination between CNR and residual CO ligand(s). For instance, carbonyl-isocyanide replacement from [M₂Cp₂(CO)₄] (M = Fe, Ru) usually generates a mixture of μ-CNR and t-CNR isomers, which interconvert in solution,^{41,50,51} and the bridging coordination is favored with electron-withdrawing R groups.^{41,52} In a series of dpmm-bridged heterobimetallic (Pt-M) μ-carbonyl complexes, CO-CNR replacement addresses isocyanides with electron-withdrawing substituents to the bridging site and isocyanides

Table 3. NBO Second-Order Perturbation Stabilization Energies ($E^{(2)}$, kcal mol⁻¹) for Donor (D) → Acceptor (A) Pairs

isomer	D → A	$E^{(2)}$
2aA	LP1(N ^A) → LV1(C ^t)	23.1
	LP1(N ^A) → BD*1(C ^t O)	0.9
	LP1(Fe ¹) → LV1(C ^t)	27.3
	LP1(Fe ¹) → BD*1(C ^t O)	4.4
	LP2(Fe ¹) → LV1(C ^t)	13.5
	LP2(Fe ¹) → BD*1(C ^t O)	16.8
2aB	LP1(Fe ¹) → LV1(C ^t)	11.6
	LP1(Fe ¹) → LV2(C ^t)	64.0
	LP2(Fe ¹) → LV1(C ^t)	45.1
	LP2(Fe ¹) → LV2(C ^t)	24.0
	LP3(Fe ¹) → LV1(C ^t)	49.9
	LP1(N ^A) → BD*1(C ^t O)	1.7
2bA	LP1(N ^A) → LV1(C ^t O)	17.9
	LP1(Fe ¹) → LV1(C ^t)	19.1
	LP1(Fe ¹) → BD*1(C ^t O)	6.7
	LP2(Fe ¹) → BD*1(C ^t O)	26.0
	LP2(N ^A) → BD*1(C ^t O)	13.5

Table 4. Gibbs Free Energy (in kcal/mol) and Descriptors for the Spatial Arrangement of 2b-Related Structures

Isomer	ΔG	Cp/Cp	R/CO	CNR
2bA	0.0	cis	cis	bridging
2bB	6.0	trans	cis	bridging
2bC	1.0	cis	trans	bridging
2bD	12.0	trans	trans	bridging
2bE	4.6	cis	cis	terminal
2bF	6.7	trans	trans	terminal

with donor substituents to one terminal site.⁵³ Note that different outcomes (bridging or terminal coordination of CNR) were observed with R = CH₂PO(OEt)₂, depending on the nature of one of the two metal centers.⁴⁰ It is noteworthy that, in tris-carbonyl aminocarbyne complexes of type **1** (Scheme 1), CO-CNR monosubstitution locates any type of isocyanides in terminal coordination,⁵⁴ while two terminal coordination sites are selectively occupied by aryl-isocyanides (with a residual μ -CO) following disubstitution reactions.⁵⁵ In **2a–c**, the isocyanide ligand is exclusively found as bridging coordinated to the two iron centers, irrespective of the electron properties of its substituent R: this appears the consequence of the intramolecular interaction favoring the terminal coordination of the CO ligand (see above).

It is reasonable that CO-CNR substitution from **1** proceeds with a dissociative mechanism since the iron atoms are coordinatively saturated. On account of the weaker metal binding of t-CO compared to that of μ -CO, the former is expected to be preferentially released upon thermal treatment, generating a coordination vacancy (structure **Int1** in Figure 2) that can be readily filled with the isocyanide. This situation was simulated using CNMe as a model isocyanide (structure **Int2**, corresponding to **2aE**; see Figure S13). Since the migration of the bridging CO to the terminal site of **Int1** is not viable, **Int2** should be the kinetic product of the substitution process; despite being less stable than **1**, the formation of **Int2** is probably pushed by the gaseous nature of released CO. A subsequent, plausible intermediate structure (**Int3**) was DFT-recognized, bearing bridging CO and CNMe ligands: its

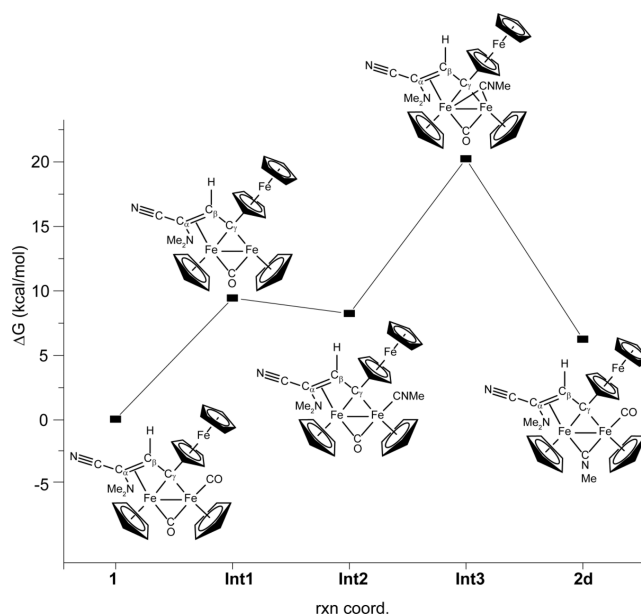


Figure 2. Gibbs energy profile of the proposed reaction pathway for carbon monoxide-isocyanide substitution from complex **1**.

energy is high but accessible at room temperature. A view of the DFT-optimized structure of **Int3** is shown in Figure S15. Then, opening of the bridging CO leads to the most stable structure **2d**, homologous to **2a**.

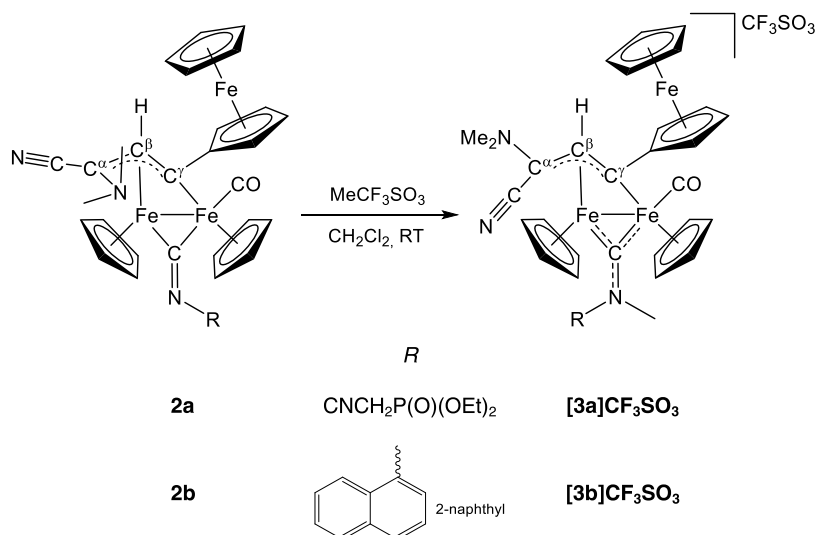
The reactions of **1** with cyclohexyl isocyanide (CNCy) and 2,6-dimethylphenyl-isocyanide (CNXyl) resulted in prevalent decomposition. It was previously demonstrated that these isocyanides react with [Fe₂Cp₂(CO)₄] to give cis and trans isomers of [Fe₂Cp₂(CO)(μ -CO)₂(CNR)], and terminal to bridging migration of the isocyanide is hampered even under high-temperature conditions.⁴¹ In particular, the steric hindrance exerted by CNXyl is mainly imputable to the two ortho-methyl groups,⁵⁶ a situation not found in naphthyl isocyanide. Thus, it is possible that CO-CNR (R = Cy, Xyl) substitution from **1** affords μ -CO intermediates analogous to **2aF**, decomposing at the high temperature required for the reaction, in the absence of a viable mechanism enabling the CNR migration from terminal to bridging site and, thus, the establishment of a stabilizing amine-terminal CO interaction. On the other hand, the stable bridging bonding of CNXyl has been demonstrated for dinuclear Fe–Pt complexes.⁵⁷

2.2. Synthesis of Aminocarbyne Ligands. Isocyanide ligands in transition-metal complexes may be prone to the addition of electrophiles to form the corresponding aminocarbyne ligands.^{20,32,43,58,59} In general, the Lewis basicity of the nitrogen atom is enhanced on increasing the electron π back-donation from the metal center(s) to the isocyanide; therefore, in dinuclear complexes, the bridging coordination may be crucial to permit the conversion into aminocarbyne.^{60–64}

In light of the presence of a bridging isocyanide ligand in the neutral complexes **2a–c**, we moved to investigate their reactivity with an easily available alkylating agent such as methyl triflate.

Hence, the reactions of **2a–b** with a slight excess of MeCF₃SO₃ were effective to produce the isocyanide-methylated products [3a–b]CF₃SO₃, which were isolated in good yields after workup (Scheme 3). Notably, the methylation of **2a–b** takes place selectively at the isocyanide: this outcome is not trivial because the allylidene fragment,

Scheme 3. Isocyanide Methylation Affording Complexes with Two Functionalized Bridging Hydrocarbyl Ligands



comprising an extensive unsaturation and two nitrogen functions, could in principle take part in the alkylation process. Spectroscopic data suggest that the methylation of **2c** was unclear, affording the corresponding aminocarbyne derivative in admixture with impurities, which could not be removed.⁶⁵

The structure of $[\text{3a}]\text{CF}_3\text{SO}_3$ was ascertained by X-ray diffraction, and a view of the structure is shown in Figure 3, while relevant bonding parameters of **1**, **2a**, and $[\text{3a}]\text{CF}_3\text{SO}_3$ are comparatively reported in Table 1. The structure of $[\text{3a}]^+$ is composed of a *cis*- Fe_2Cp_2 core bonded to a $\mu\text{-}\eta^1\text{:}\eta^3\text{-}$

$\text{C}(\text{Fc})\text{CHC}(\text{CN})\text{NMe}_2$ allylidene, a $\mu\text{-CN}(\text{Me})\text{CH}_2\text{P}(\text{O})(\text{OEt})_2$ aminocarbyne, and a terminal CO ligand. Notably, the configuration of the NMe_2 and CN groups at C(2) of $[\text{3a}]^+$ is inverted compared to the parent compound **2a**. Apart from this, the bond distances related to the bridging allylidene are very similar in $[\text{3a}]^+$ and **2a**, as well as **1** (Table 1). The transformation of the bridging isocyanide into bridging aminocarbyne ligand causes the shortening of both $\text{Fe}(1)\text{-C}(11)$ and $\text{Fe}(2)\text{-C}(11)$ bonds, passing from **2a** [1.962(11) and 1.927(10) Å, respectively] to $[\text{3a}]^+$ [1.899(7) and 1.878(6) Å], whereas $\text{C}(11)\text{-N}(2)$ [1.202(13) Å in **2a**; 1.292(9) Å in $[\text{3a}]^+$] is sensibly elongated. These data are in keeping with the bonding parameters previously reported for related diiron complexes containing bridging aminocarbyne ligands.^{20,66} It is remarkable that the isocyanide methylation is accompanied by an apparent inversion of orientation of the $\text{CH}_2\text{P}(\text{O})(\text{OEt})_2$ substituent.

Based on X-ray data, the bridging (hetero)hydrocarbyl ligand derived from isocyanide methylation in $[\text{3a-b}]^+$ may be viewed as a hybrid between aminocarbyne and iminium structures (Scheme 4), analogously to the description of several dimetallic aminocarbyne complexes in the literature.²⁰ Note that aminocarbyne ligands commonly adopt bridging coordination in polymetallic carbonyl complexes due to the strong electron-withdrawing character of the aminocarbyne exceeding that of carbon monoxide.^{67,68}

The structure of the cation $[\text{3a}]^+$ was optimized by DFT calculations (**3aA**), leading to a similar geometry to that experimentally determined, with the Me_2N group not oriented toward the terminal CO ligand. Isomers of **3aA** are theoretically predictable, and in particular **3aB**, containing the methylphosphonate group on the same side with respect to the CO ligand, and **3aC**, displaying the Me_2N moiety pointing toward the CO (see Figure S16). Thus, **3aB** resulted in 1.2 kcal/mol less stable than **3aA**, presumably due to small steric differences, while **3aC** is less stable than **3aA** by only 1.7 kcal/mol. Although the stereoisomers **3aA**, **3aB**, and **3aC** are energetically similar, their interconversion is not obvious, and therefore the inversion of configuration at C^α and CNR during the methylation of **2a** is not easy to explain. In particular, C_α is bound to three carbon atoms (bond orders 1.08, 1.04, and 1.06 in **3aA**) and one iron (bond order 0.65); thus, we hypothesize

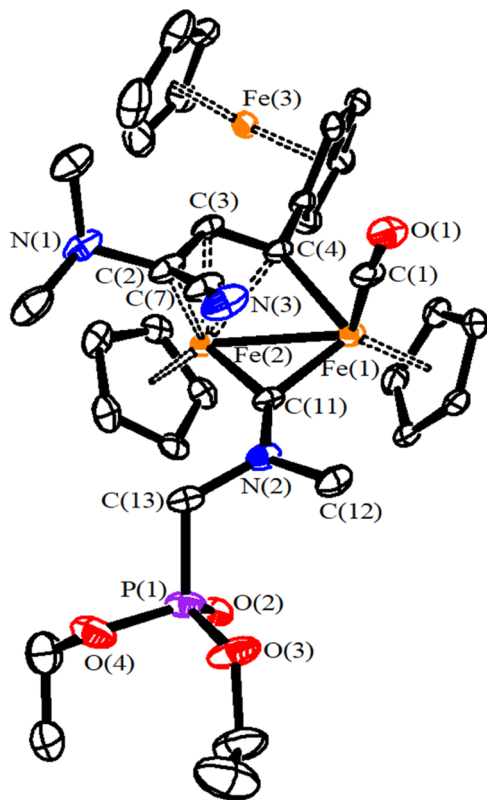
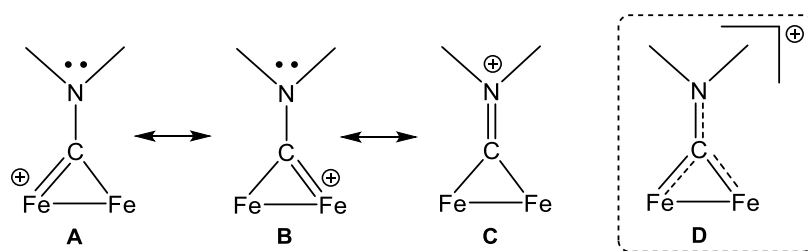


Figure 3. View of the molecular structure of $[\text{3a}]^+$. Displacement ellipsoids are at the 30% probability level. H atoms have been omitted for clarity.

Scheme 4. Aminocarbyne (A, B) and Iminium (C) Canonical Forms for the Bridging Ligand Derived from Isocyanide Alkylation in the Diiron Complexes $[3a-b]^+$ and Representative Delocalized Structure (D)



that the inversion of configuration at C^α proceeds via intermediate species in which the $C^\alpha-C^\beta-C^\gamma$ chain adopts a significantly different coordination to the diiron scaffold. Note that bridging allylidene ligands might exhibit fluxional behavior under certain conditions.^{69,70} No NBO $D \rightarrow A$ interaction between the $C^\alpha-CN$ unit and the terminal carbonyl was found in **3aA**, the distance between N(3) and C(1) (2.912 Å) being too long. Conversely, in **3aC**, the interaction between the Me_2N unit and the terminal carbonyl is allowed, the NBO analysis leading to $LP1(N^A) \rightarrow LV\ 1(C^t)$ with $E^{(2)} = 32.25$ kcal/mol. However, in **3aC**, there is a relevant steric hindrance between Me_2N and the aminocarbyne, which disfavors this isomer with respect to **3aA**.

The spectroscopic data of $[3a-b]CF_3SO_3$ are in alignment with the above considerations concerning the structure of $[3a]^+$. Thus, the IR spectra display absorptions ascribable to the C^α -bound cyano group (at 2192 cm^{-1}), the terminal carbonyl ($\sim 50\text{ cm}^{-1}$ shifted to higher wavenumbers with respect to **2a-b** because of the net positive charge acquired by $[3a-b]CF_3SO_3$), and the $\mu-CN$ moiety (at $1541\text{--}1552\text{ cm}^{-1}$). The latter values fall within the interval of C–N bonds in bridging aminocarbyne complexes (Scheme 4).^{20,71}

The NMR spectra of $[3a-b]CF_3SO_3$ show the presence of two isomers in solution, one of them being largely predominant. Based on the DFT outcomes, it is probable that such pairs of isomers differ in the orientation of the substituents on the aminocarbyne moiety (E and Z isomers). Accordingly, the signals related to the aminocarbyne methyl differ significantly in the two isomers (e.g., at 5.16 and 4.49 ppm in the 1H NMR spectrum of **3b**). In both complexes, the salient spectroscopic feature is the ^{13}C NMR resonance of the bridging $\{\mu-CN\}$ carbon, falling at approximately 327 ppm, in full alignment with the aminocarbyne nature.²⁰

The inversion of the stereochemical configuration at the C^α determines a significant effect on the adjacent $\{C^\beta-H\}$ group, which experiences a substantial downfield shift. For instance, the related NMR signals fall at 6.27 (1H) and 76.6 ppm (^{13}C) in $[3a]CF_3SO_3$ and at 5.42 and 63.5 ppm in the parent compound **2a** (Table S1). Similar chemical shift variations regard the C^α and C^γ carbons within the C_3 chain of the allylidene ligand. Key information provided by NMR spectra concerns the amine group since the two methyl groups resonate as a unique singlet, e.g., at 2.55 ppm (1H) and 44.7 ppm (^{13}C) for the major isomer of $[3a]CF_3SO_3$. This feature confirms that the rotation around the $C^\alpha-N$ bond is permitted in $[3a-b]^+$, coherently with the stereochemical configuration of C^α revealed by the X-ray structure of $[3a]CF_3SO_3$. The ^{31}P resonance for the phosphonate shifts from 24.0 to 19.8 ppm on going from **2a** to $[3a]CF_3SO_3$.

In summary, complexes $[3a]CF_3SO_3$ show the coexistence of two functionalized hydrocarbyl bridging ligands, constructed

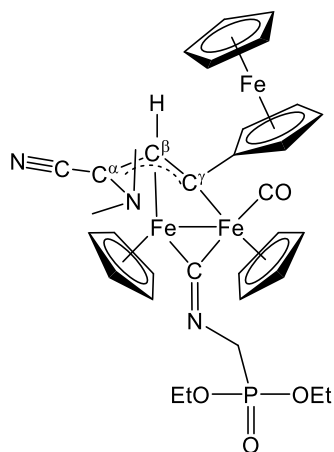
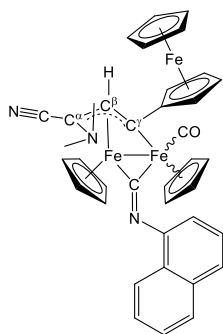
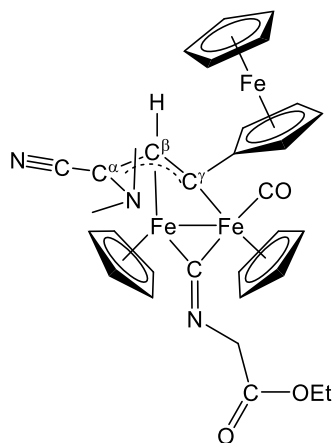
from $[Fe_2Cp_2(CO)_4]$ through the progressive elimination of three carbonyl ligands and the assembly of small organic units and, in this respect, they break the most common scheme whereby the growth of an organometallic architecture in a dinuclear metal complex is centered on a single bridging site.⁷² Looking back at Scheme 1, the C_1 to C_3 growing on a diiron platform, starting from an aminocarbyne ligand (structure I), is followed by the construction of a second aminocarbyne affecting the stereochemistry of the C_3 fragment.

3. CONCLUSIONS

We carried out a synthetic work aimed to explore the reactivity of a diiron scaffold with a bridging functionalized ferrocenyl-allylidene ligand, leading to the two-step formation of an additional aminocarbyne ligand by the assembly of CNR and Me^+ units. The construction of the aminocarbyne moiety is highly selective, in that the allylidene fragment is not directly involved, despite the potential reactivity associated with its extensive unsaturation and the presence of amine and cyano groups. On the other hand, the allylidene is sensitive to the structural modifications on the other side of the dimetallic framework and plays a crucial role in the selectivity of the process by means of the stabilizing intramolecular interaction with the terminal CO and the subsequent inversion of configuration at one allylidene carbon. The finally obtained allylidene-aminocarbyne complexes represent remarkable examples of dimetallic species comprising two functionalized hydrocarbyl ligands, which occupy two bridging coordination sites (two-faced). Our results demonstrate the potency of cooperative effects mediated by the $\{Fe_2Cp_2\}$ core and exalted—rather than hindered—by the preliminary formation of one bridging structured ligand, thus confirming the versatility of diiron carbonyl systems for synthetic purposes.

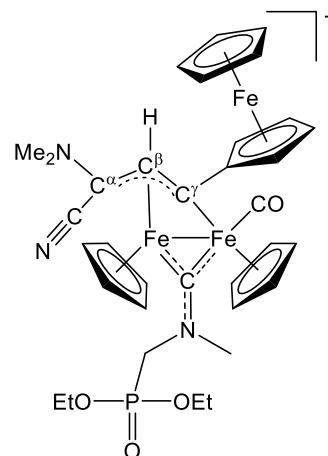
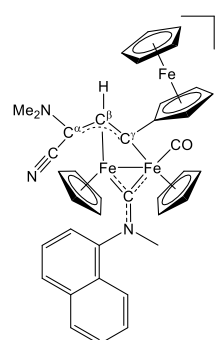
4. EXPERIMENTAL SECTION

4.1. General Experimental Details. **4.1.1. Materials and Methods.** Reactants and solvents were purchased from Alfa Aesar, Merck, Strem, or TCI Chemicals and were of the highest purity available. Complex **1** was prepared according to the literature procedure.³⁸ Reactions were conducted under a N_2 atmosphere using standard Schlenk techniques and monitored by liquid IR spectroscopy. Products were conserved under a N_2 atmosphere once isolated. Dichloromethane, tetrahydrofuran, and diethyl ether were dried with the solvent purification system mBraun MB SPSS, while isopropanol was deaerated by bubbling N_2 into the liquid (ca. 2 L) for 20 min. Chromatography separations were carried out under a flux of N_2 on columns of deactivated alumina (Merck, 4% w/w water) using solvents from the bottle. IR spectra of solutions were recorded using a CaF_2 liquid transmission cell ($2300\text{--}1500\text{ cm}^{-1}$) on a Perkin Elmer Spectrum 100 FT-IR spectrometer. IR spectra were processed with Spectragryph software.⁷³ NMR spectra were recorded at 298 K on a Jeol JNM-ECZ500R instrument equipped with a Royal HFX

Chart 1. Structure of **2a**Chart 2. Structure of **2b**Chart 3. Structure of **2c**

Broadband probe. Chemical shifts (expressed in parts per million) are referenced to the residual solvent peaks⁷⁴ or to an external standard (³¹P to 85% H₃PO₄). NMR spectra were assigned with the assistance of ¹H–¹³C (gs-HSQC and gs-HMBC) correlation experiments.⁷⁵ NMR signals due to secondary isomeric forms (where it has been possible to detect them) are italicized. Elemental analyses were performed on a Vario MICRO cube instrument (Elementar).

4.2. Synthesis and Characterization of Allylidene Isocyanide Complexes. General procedure. A solution of complex **1** in isopropanol (ca. 15 mL) was treated with the selected isocyanide, and the resulting solution was stirred at ca. 100 °C for ca. 2 h. Then, the volatiles were removed under vacuum, and the residue was dissolved in the minimum volume of diethyl ether. This solution was charged on an alumina column packed with petroleum ether. The fraction containing the product was dried under vacuum affording a solid

Chart 4. Structure of [**3a**]⁺Chart 5. Structure of [**3b**]⁺

residue. In the case of **2a**, prior chromatography and in order to remove the excess of isocyanide, the reaction mixture was concentrated to ca. 5 mL, and Et₂O (15 mL) and H₂O (15 mL) were added and vigorously shaken. The organic phase was separated, and the extraction procedure was repeated twice. The final organic solution was directly charged on the alumina column (Chart 1).

4.2.1. [*Fe*₂Cp₂(CO){μ-CNCH₂P(O)(OEt)₂}[μ-η¹:η³-C'(Fc)C^βHC^α(CN)-NMe₂]], **2a** (Chart 1). From **1** (120 mg, 0.203 mmol) and diethyl isocyanomethylphosphonate (2.5 equiv). Eluent for chromatography: THF. Brown solid, yield 105 mg (70%). Anal. calcd. for C₃₃H₃₈Fe₃N₃O₄P: C, 53.62; H, 5.18; N, 5.68. Found: C, 53.51; H, 5.26; N, 5.49. IR (CH₂Cl₂): $\tilde{\nu}$ /cm⁻¹ = 2186w (C≡N), 1958s (CO), 1705m (μ-C≡N). ¹H NMR (CDCl₃): δ/ppm = 5.42 (s, 1H, C^βH); 4.75, 4.64 (s, 10H, Cp); 4.51, 4.47, 4.40 (m, 4H, C₅H₄); 4.33 (s, 5H, Cp^{Fc}); 4.10, 4.08 (d, ²J_{HH} = 14.5 Hz, 2H, NCH₂); 4.24 (m, 2H, CH₂CH₃); 2.27, 1.75 (s, 6H, NMe₂); 1.49, 1.42 (t, 6H, CH₂CH₃). ¹³C{¹H} NMR (CDCl₃): δ/ppm = 258.0 (μ-CN); 213.4 (CO); 196.8 (C^γ); 121.1 (C≡N); 112.9 (ipso-C₅H₄); 83.7 (C^β); 88.6, 86.3 (Cp); 72.6, 67.3, 67.1, 67.0 (C₅H₄); 69.2 (Cp^{Fc}); 64.1 (d, J = 26 Hz, NCH₂); 63.5 (C^α); 62.9, 62.3 (d, CH₂CH₃); 50.3, 41.5 (NMe₂); 16.9 (CH₂CH₃). ³¹P{¹H} NMR (CDCl₃): δ/ppm = 24.0.⁷⁶ Crystals suitable for X-ray analysis were obtained by the slow diffusion of heptane into a solution of **2a** in CH₂Cl₂, at -30 °C (Chart 2).

4.2.2. [*Fe*₂Cp₂(CO){μ-CN(2-Naphthyl)}[μ-η¹:η³-C'(Fc)C^βHC^α(CN)-NMe₂]], **2b** (Chart 2). From **1** (90 mg, 0.153 mmol) and 2-naphthyl isocyanide (2.5 equiv). Eluent for chromatography: Et₂O. Brown solid, yield 92 mg (84%). Anal. calcd. for C₃₈H₃₃Fe₃N₃O: C, 63.81; H, 4.65; N, 5.88. Found: C, 63.65; H, 4.75; N, 5.89. IR (CH₂Cl₂): $\tilde{\nu}$ /cm⁻¹ = 2187w (C≡N), 1961s (CO), 1703m (μ-C≡N). ¹H NMR (CDCl₃): δ/ppm = 7.84–7.40 (m, 7H, C₁₀H₇); 5.38 (s, 1H, C^βH); 4.88, 4.84, 4.54, 4.37 (s, 10H, Cp), 5.01, 4.75, 4.61, 4.46 (br, 4H, C₅H₄); 4.26 (s, 5H, Cp^{Fc}); 2.55, 2.27, 1.98, 1.85 (s, 6H, NMe₂). Isomer ratio (cis/trans) = 5. ¹³C{¹H} NMR (CDCl₃): δ/ppm = 252.6 (μ-CN); 214.5 (CO); 197.6 (C^γ); 144.6 (ipso-C₁₀H₇); 134.5, 130.3,

Table 5. Crystal Data and Measurement Details for 2a·CH₂Cl₂ and [3a]CF₃SO₃·H₂O

	2a·CH ₂ Cl ₂	[3a]CF ₃ SO ₃ ·H ₂ O
formula	C ₃₄ H ₄₀ Cl ₂ Fe ₃ N ₃ O ₄ P	C ₃₅ H ₄₃ F ₃ Fe ₃ N ₃ O ₈ PS
FW	824.11	921.30
T, K	100(2)	100(2)
λ, Å	0.71073	0.71073
crystal system	triclinic	triclinic
space group	P $\bar{1}$	P $\bar{1}$
a, Å	9.8976(18)	11.9074(7)
b, Å	14.069(3)	13.4740(8)
c, Å	14.208(3)	13.8818(8)
α, deg	66.748(7)	108.046(2)
β, deg	88.160(7)	102.104(2)
γ, deg	72.599(7)	111.591(2)
cell volume, Å ³	1726.1(6)	1832.34(19)
Z	2	2
D _c , g·cm ⁻³	1.586	1.670
μ, mm ⁻¹	1.488	1.344
F(000)	848	948
crystal size, mm	0.15 × 0.11 × 0.08	0.18 × 0.15 × 0.10
θ limits, deg	1.568–25.000	1.658–25.100
reflections collected	10,579	18,978
independent reflections	6003 [R _{int} = 0.0706]	6507 [R _{int} = 0.0599]
data/restraints/parameters	6003/132/428	6507/365/486
goodness on fit on F ²	1.076	1.034
R ₁ (I > 2σ(I))	0.1055	0.0845
wR ₂ (all data)	0.2966	0.2318
largest diff. peak and hole, e Å ⁻³	2.557/−1.267	1.671/−1.162

129.1, 127.9, 127.6, 126.4, 125.6, 124.5, 116.5 (C₁₀H₇); 121.9 (C≡N); 112.1 (ipso-C₅H₄); 88.6, 88.4, 87.3, 85.7 (Cp); 82.9 (C^β); 72.6, 68.1, 67.6, 67.1 (C₅H₄); 69.3 (Cp^{Fc}); 65.9 (C^α); 50.6, 42.4 (NMe₂) (Chart 3).

4.2.3. [Fe₂Cp₂(CO){μ-CNCH₂C(O)(OEt)}{μ-η¹:η³-C'(Fc)C^βHC^α(CN)-NMe₂}], 2c (Chart 3). From 1 (64 mg, 0.109 mmol) and ethyl 2-isocyanoacetate (4.0 equiv). Eluent for chromatography: Et₂O/CH₂Cl₂ 9:1 v/v. Brown solid, yield 45 mg (61%). Anal. calcd. for C₃₂H₃₃Fe₃N₃O₃: C, 56.93; H, 4.93; N, 6.22. Found: C, 56.83; H, 5.02; N, 6.15. IR (CH₂Cl₂): $\tilde{\nu}$ /cm⁻¹ = 2186w (C≡N), 1957s (CO), 1723m (OCO), 1711m (μ-C≡N). ¹H NMR (CDCl₃): δ/ppm = 5.41 (s, 1H, C^βH); 4.79, 4.56 (s, 10H, Cp); 4.54, 4.49, 4.41, 4.23 (m, 4H, C₅H₄); 4.62, 4.43 (d, ²J_{HH} = 16.7 Hz, 2H, NCH₂); 4.34 (s, 5H, Cp^{Fc}); 4.31 (q, ³J_{HH} = 7.07 Hz, 2H, CH₂CH₃); 2.30, 1.77 (s, 6H, NMe₂); 1.36 (t, 3H, CH₂CH₃). ¹³C{¹H} NMR (CDCl₃): δ/ppm = 257.3 (μ-CN); 213.4 (CO); 196.6 (C^γ); 171.2 (CO₂Et); 120.9 (C≡N); 112.8 (ipso-C₅H₄); 88.3, 86.6 (Cp); 83.7 (C^β); 72.7, 69.1, 67.4, 67.1 (C₅H₄); 69.3 (Cp^{Fc}); 64.1 (C^α); 61.4 (CH₂CH₃); 59.8 (NCH₂); 50.4, 41.6 (NMe₂); 15.4 (CH₂CH₃).

4.3. Synthesis and Characterization of Allylidene–Amino-carbyne Complexes. 4.3.1. General Procedure. The appropriate isocyanide complex, 2a–b, was dissolved in CH₂Cl₂, and this solution was treated with CH₃SO₃CF₃ (ca. 1.5 equiv). The resulting mixture was stirred at room temperature for 2 h, during which a progressive color turning from brown to green was observed. The final product was purified by alumina chromatography, and a green band was collected. Purification of [3a]CF₃SO₃ was performed by washing the solid with diethyl ether and subsequent filtration through celite of a dichloromethane solution, while purification of [3b]CF₃SO₃ was achieved via alumina chromatography. Removal of the volatiles under vacuum from the respective solutions allowed us to isolate the products as dark-green powders (Chart 4).

4.3.2. [Fe₂Cp₂(CO){μ-CN(Me)CH₂C(O)(OEt)}{μ-η¹:η³-C'(Fc)-C^βHC^α(CN)NMe₂}]CF₃SO₃, [3a]CF₃SO₃ (Chart 4). From 2a (105 mg, 0.142 mmol). Dark-green solid, yield 95 mg (74%). Anal. calcd. for C₃₄H₃₆F₃Fe₃N₃O₆S: C, 48.66; H, 4.32; N, 5.01; S, 3.82. Found: C, 48.75; H, 4.22; N, 4.96; S, 3.69. IR (CH₂Cl₂): $\tilde{\nu}$ /cm⁻¹ = 2192w (C≡

N), 2012s (CO), 1552m (μ-CN). ¹H NMR (acetone-*d*₆): δ/ppm = 6.34, 6.27 (s, 1H, C^βH); 5.62, 5.56, 5.30, 5.28 (s, 10H, Cp); 5.06, 4.78, 4.66, 4.58 (m, 4H, C₅H₄); 4.51, 4.50 (s, 5H, Cp^{Fc}); 4.92, 4.12 (s, 3H, NMe); 4.48–4.34 (m, 4H, OCH₂); 4.92 (m, 2H, NCH₂); 2.66, 2.55 (s, 6H, NMe₂); 1.49, 1.40 (t, 6H, CH₂CH₃). Isomer ratio = 4. ¹³C{¹H} NMR (acetone-*d*₆): δ/ppm = 327.6, 327.5 (μ-CN); 210.1 (CO); 207.8 (C^γ); 112.1 (ipso-C₅H₄); 93.5, 88.3, 88.0 (Cp); 90.9, 89.1 (C^β); 76.6 (C^α); 73.8, 73.5, 69.4, 69.3, 68.6, 68.4, 67.2 (C₅H₄); 70.0, 69.9 (Cp^{Fc}); 69.9 (NCH₂); 63.5 (d, CH₂CH₃); 56.7, 52.7 (NMe); 44.7 (br, NMe₂); 16.1 (CH₂CH₃). ³¹P{¹H} NMR (acetone-*d*₆): δ/ppm = 19.8, 16.5. Crystals suitable for X-ray analysis were obtained by the slow diffusion of diethyl ether into a solution of [3a]CF₃SO₃ in methanol at −30 °C (Chart 5).

4.3.3. [Fe₂Cp₂(CO){μ-CN(Me)(2-Naphthyl)}{μ-η¹:η³-C'(Fc)-C^βHC^α(CN)NMe₂}]CF₃SO₃, [3b]CF₃SO₃ (Chart 5). From 2b (37 mg, 0.052 mmol). Eluent for chromatography: MeCN. Dark-green solid, yield 31 mg (68%). Anal. calcd. for C₄₀H₃₆F₃Fe₃N₃O₄S: C, 54.64; H, 4.13; N, 4.78; S, 3.65. Found: C, 54.46; H, 4.04; N, 4.86; S, 3.56. IR (CH₂Cl₂): $\tilde{\nu}$ /cm⁻¹ = 2192w (C≡N), 2007s (CO), 1597w, 1541m (μ-CN). ¹H NMR (acetone-*d*₆): δ/ppm = 8.22–7.29 (m, 7H, C₁₀H₇); 6.44, 6.28 (s, 1H, C^βH); 5.76, 5.43, 4.53, 4.53, 4.51, 4.48 (s, 15H, Cp); 5.00, 4.94, 4.76, 4.74, 4.67, 4.63, 4.61, 4.58 (m, 4H, C₅H₄); 5.16, 4.49 (s, 3H, NMe); 2.68, 2.43 (s, 6H, NMe₂). Isomer ratio = 6. ¹³C{¹H} NMR (acetone-*d*₆): δ/ppm = 326.2 (μ-CN); 210.7 (CO); 207.7 (C^γ); 143.1 (ipso-C₁₀H₇); 133.6, 133.4, 133.7, 130.9, 130.7, 128.6, 128.4, 128.3, 128.1, 128.0, 127.9, 127.7, 127.6, 127.5, 123.9, 123.8, 115.9, 114.5 (C₁₀H₇); 122.7, 122.6 (C≡N); 111.7, 111.4 (ipso-C₅H₄); 93.9, 93.2, 88.5, 88.2 (Cp); 91.1, 89.9 (C^β); 75.3 (C^α); 73.6, 73.1, 69.5, 69.2, 68.5, 68.4, 67.2, 66.9 (C₅H₄); 73.6, 69.9 (Cp^{Fc}); 56.0 (NMe); 45.2, 44.8 (NMe₂).

4.4. X-ray Crystallography. Crystal data and collection details for 2a·CH₂Cl₂ and [3a]CF₃SO₃·H₂O are reported in Table 5. Data were recorded on a Bruker APEX II diffractometer equipped with a PHOTON2 detector using Mo-Kα radiation. The structures were solved by direct methods and refined by full-matrix least-squares based on all data using F².⁷⁷ Hydrogen atoms were fixed at calculated positions and refined isotropically using a riding model. The structure

of $[3a]CF_3SO_3 \cdot H_2O$ presents some minor disorders mainly concerning the $CF_3SO_3^-$ anion, the unsubstituted Cp rings, and the Et groups of the cation. Such a disorder is rather common for such groups.

4.5. DFT Calculations. All geometries were optimized with ORCA 5.0.1 using the B97 functional⁷⁸ in conjunction with a single- ζ quality basis set (def2-sVP).⁷⁹ To reduce the computational effort, the EtO units in **2a** and $[3a]^+$ were replaced by MeO units due to the similar electronic properties and peripheral location of these groups. The dispersion corrections were introduced using the Grimme D3-parameterized correction and the Becke–Johnson damping to the DFT energy.⁸⁰ All of the structures were confirmed to have no imaginary frequencies. The final energy has been computed with a single-point calculation using a triple- ζ quality basis set (def2-TZVP).⁷⁹ The polar environment of the ionic crystal lattice solvent was considered through the continuum-like polarizable continuum model (isopropanol). Anyway, it has been verified that the ΔG between different isomers does not depend on solvent correction. Natural bond analysis (NBO) has been performed using the NBO 7.0 suite of software.⁸¹

■ ASSOCIATED CONTENT

SI Supporting Information

The Supporting Information is available free of charge at <https://pubs.acs.org/doi/10.1021/acs.organomet.3c00088>.

Comparative view of spectroscopic data (Table S1); NMR spectra of products (Figures S1–S12); and DFT studies (Figures S13–S16) (PDF)

Cartesian coordinates of the DFT-optimized structures (XYZ)

Accession Codes

CCDC 2237478–2237479 contain the supplementary crystallographic data for this paper. These data can be obtained free of charge via www.ccdc.cam.ac.uk/data_request/cif, or by emailing data_request@ccdc.cam.ac.uk, or by contacting The Cambridge Crystallographic Data Centre, 12 Union Road, Cambridge CB2 1EZ, UK; fax: +44 1223 336033.

CCDC reference numbers 2237478 (**2a**) and 2237479 ($[3a]CF_3SO_3$) contain the supplementary crystallographic data for the X-ray studies reported in this paper. These data can be obtained free of charge at <https://www.ccdc.cam.ac.uk/structures/> or from the Cambridge Crystallographic Data Centre, 12, Union Road, Cambridge CB2 1EZ, UK; e-mail: deposit@ccdc.cam.ac.uk.

■ AUTHOR INFORMATION

Corresponding Authors

Gianluca Ciancaleoni – Dipartimento di Chimica e Chimica Industriale, University of Pisa, I-56124 Pisa, Italy;

orcid.org/0000-0001-5113-2351;

Email: gianluca.ciancaleoni@unipi.it

Fabio Marchetti – Dipartimento di Chimica e Chimica Industriale, University of Pisa, I-56124 Pisa, Italy;

orcid.org/0000-0002-3683-8708;

Email: fabio.marchetti@unipi.it

Authors

Chiara Zappelli – Dipartimento di Chimica e Chimica Industriale, University of Pisa, I-56124 Pisa, Italy

Stefano Zacchini – Dipartimento di Chimica Industriale “Toso Montanari”, University of Bologna, I-40136 Bologna, Italy; orcid.org/0000-0003-0739-0518

Complete contact information is available at:

<https://pubs.acs.org/10.1021/acs.organomet.3c00088>

Author Contributions

C.Z.: synthesis and characterization of complexes; G.C.: DFT calculations and writing; S.Z.: X-ray analyses; and F.M.: design of the synthetic work, supervision, and writing.

Notes

The authors declare no competing financial interest.

■ ACKNOWLEDGMENTS

The authors thank the University of Pisa for financial support (Fondi di Ateneo 2021).

■ REFERENCES

- (1) Pal, S.; Uyeda, C. Evaluating the Effect of Catalyst Nuclearity in Ni-Catalyzed Alkyne Cyclotrimerizations. *J. Am. Chem. Soc.* **2015**, *137*, 8042–8045.
- (2) Patra, S.; Maity, N. Recent advances in (hetero)dimetallic systems towards tandem catalysis. *Coord. Chem. Rev.* **2021**, *434*, No. 213803.
- (3) Li, G.; Zhu, D.; Wang, X.; Su, Z.; Bryce, M. R. Dinuclear metal complexes: multifunctional properties and applications. *Chem. Soc. Rev.* **2020**, *49*, 765–838.
- (4) Karunananda, M. K.; Mankad, N. P. E- Selective Semi-Hydrogenation of Alkynes by Heterobimetallic Catalysis. *J. Am. Chem. Soc.* **2015**, *137*, 14598–14601.
- (5) Liu, Y.; Zhou, G.; Zhang, Z.; Lei, H.; Yao, Z.; Li, J.; Lin, J.; Cao, R. Significantly improved electrocatalytic oxygen reduction by an asymmetrical Pacman dinuclear cobalt(II) porphyrin – porphyrin dyad. *Chem. Sci.* **2020**, *11*, 87–96.
- (6) van den Beuken, E. K.; Feringa, B. L. Bimetallic catalysis by late transition metal complexes. *Tetrahedron* **1998**, *54*, 12985–13011.
- (7) Ritleng, V.; Chetcuti, M. J. Hydrocarbyl Ligand Transformations on Heterobimetallic Complexes. *Chem. Rev.* **2007**, *107*, 797–858.
- (8) Wigginton, J. R.; Chokshi, A.; Graham, T. W.; McDonald, R.; Ferguson, M. J.; Cowie, M. Alkyne/Methylene Coupling Reactions at Adjacent Rh/Os Centers: Stepwise Transformations from C1-through C4-Bridged Species. *Organometallics* **2005**, *24*, 6398–6410.
- (9) Bruce, G. C.; Gangnus, B.; Garner, S. E.; Knox, S. A. R.; Guy Orpen, A.; Phillips, A. J. Vinyl Homologation via Methyl Migration to p-Vinyl at a Diruthenium Centre. *J. Chem. Soc. Chem. Commun.* **1989**, 1360–1362.
- (10) Knox, S. A. R. C-C Bond Formation at Polynuclear Metal Centers. *J. Cluster Sci.* **1992**, *3*, 385–396.
- (11) Mazzoni, R.; Salmi, M.; Zanotti, V. C-C Bond Formation in Diiron Complexes. *Chem. - Eur. J.* **2012**, *18*, 10174–10194.
- (12) Bresciani, G.; Zacchini, S.; Pampaloni, G.; Marchetti, F. Carbon – Carbon Bond Coupling of Vinyl Molecules with an Allenyl Ligand at a Diruthenium Complex. *Organometallics* **2022**, *41*, 1006–1014.
- (13) Provinciali, G.; Bortoluzzi, M.; Funaioli, T.; Zacchini, S.; Campanella, B.; Pampaloni, G.; Marchetti, F. Tetrasubstituted Selenophenes from the Stepwise Assembly of Molecular Fragments on a Diiron Frame and Final Cleavage of a Bridging Alkylidene. *Inorg. Chem.* **2020**, *59*, 17497–17508.
- (14) Collins, L. R.; van Gastel, M.; Neese, F.; Fürstner, A. Enhanced Electrophilicity of Heterobimetallic Bi – Rh Paddlewheel Carbene Complexes: A Combined Experimental, Spectroscopic, and Computational Study. *J. Am. Chem. Soc.* **2018**, *140*, 13042–13055.
- (15) Chen, J.; Wang, R. Remarkable reactions of cationic carbyne complexes of manganese, rhenium, and diiron with carbonylmetal anions. *Coord. Chem. Rev.* **2002**, *231*, 109–149.
- (16) Busetto, L.; Marchetti, F.; Mazzoni, R.; Salmi, M.; Zacchini, S.; Zanotti, V. [3+2+1] cycloaddition involving alkynes, CO and bridging vinyliminium ligands in diiron complexes: a dinuclear version of the Dötz reaction? *Chem. Commun.* **2010**, *46*, 3327–3329.
- (17) Alvarez, B.; Alvarez, M. A.; Garcia, M. E.; Garcia-Vivó, D.; Ruiz, M. A. C-C and C-N Couplings Following Hydride Addition on Isocyanide Cyclopolyenyl Dimolybdenum Complexes to Give

- Tethered Aldimine and Aminocarbene Derivatives. *Chem. - Eur. J.* **2017**, *23*, 14027–14038.
- (18) Pétilion, F. Y.; Schollhammer, P.; Talarmin, J. Recent advances in the chemistry of tris(thiolato) bridged cyclopentadienyl dimolybdenum complexes. *Coord. Chem. Rev.* **2017**, *331*, 73–92.
- (19) García, M. E.; García-Vivó, D.; Ramos, A.; Ruiz, M. A. Phosphinidene-bridged binuclear complexes. *Coord. Chem. Rev.* **2017**, *330*, 1–36.
- (20) Biancalana, L.; Marchetti, F. Aminocarbene ligands in organometallic chemistry. *Coord. Chem. Rev.* **2021**, *449*, No. 214203.
- (21) Hudson, R. D. A.; Manning, A. R.; Gallagher, J. F.; Garcia, M. H.; Lopes, N.; Asselberghs, I.; Van Boxel, R.; Persoons, A.; Lough, A. J. Chiral organometallic chromophores for nonlinear optics derived from $[\text{Fe}_2(\eta^3\text{-C}_3\text{H}_5)_2(\text{CO})_2(\mu\text{-CO})(\mu\text{-C-CH}_3)][\text{BF}_4]$. *J. Organomet. Chem.* **2002**, *655*, 70–88.
- (22) Shafikov, M. Z.; Pander, P.; Zaytsev, A. V.; Daniels, R.; Martinscroft, R.; Dias, F. B.; Williams, J. A. G.; Kozhevnikov, V. N. Extended ligand conjugation and dinuclearity as a route to efficient platinum-based near-infrared (NIR) triplet emitters and solution-processed NIR-OLEDs. *J. Mater. Chem. C* **2021**, *9*, 127–135.
- (23) Campanella, B.; Braccini, S.; Bresciani, G.; De Franco, M.; Gandin, V.; Chiellini, F.; Pratesi, A.; Pampaloni, G.; Biancalana, L.; Marchetti, F. The choice of μ -vinyliminium ligand substituents is key to optimize the antiproliferative activity of related diiron complexes. *Metallomics* **2023**, *15*, No. mfac096. and references therein
- (24) Rana, S.; Prasad Biswas, J.; Paul, S.; Paik, A.; Maiti, D. Organic synthesis with the most abundant transition metal–iron: from rust to multitasking catalysts. *Chem. Soc. Rev.* **2021**, *50*, 243–472.
- (25) Fürstner, A. Iron Catalysis in Organic Synthesis: A Critical Assessment of What It Takes To Make This Base Metal a Multitasking Champion. *ACS Cent. Sci.* **2016**, *2*, 778–789.
- (26) Wang, Y.; Zhu, J.; Durham, A. C.; Lindberg, H.; Wang, Y.-M. α -C–H Functionalization of π -Bonds Using Iron Complexes: Catalytic Hydroxyalkylation of Alkynes and Alkenes. *J. Am. Chem. Soc.* **2019**, *141*, 19594–19599.
- (27) Kleinhaus, J. T.; Wittkamp, F.; Yadav, S.; Siegmund, D.; Apfel, U.-P. [FeFe]-Hydrogenases: maturation and reactivity of enzymatic systems and overview of biomimetic models. *Chem. Soc. Rev.* **2021**, *50*, 1668–1784.
- (28) Marchetti, F. Constructing Organometallic Architectures from Aminoalkylidene Diiron Complexes. *Eur. J. Inorg. Chem.* **2018**, *2018*, 3987–4003.
- (29) Bresciani, G.; Schoch, S.; Biancalana, L.; Zacchini, S.; Bortoluzzi, M.; Pampaloni, G.; Marchetti, F. Cyanide–alkene competition in a diiron complex and isolation of a multisite (cyano)alkylidene–alkene species. *Dalton Trans.* **2022**, *51*, 1936–1945.
- (30) Albano, V. G.; Busetto, L.; Marchetti, F.; Monari, M.; Zacchini, S.; Zanotti, V. C–C bond formation by cyanide addition to dinuclear vinyliminium complexes. *J. Organomet. Chem.* **2006**, *691*, 4234–4243.
- (31) Schoch, S.; Batchelor, L. K.; Funaioli, T.; Ciancaleoni, G.; Zacchini, S.; Braccini, S.; Chiellini, F.; Biver, T.; Pampaloni, G.; Dyson, P. J.; Marchetti, F. Diiron Complexes with a Bridging Functionalized Alkylidene Ligand: Synthesis, Structural Aspects, and Cytotoxicity. *Organometallics* **2020**, *39*, 361–373.
- (32) Boyarskiy, V. P.; Bokach, N. A.; Luzyanin, K. V.; Kukushkin, V. Yu. Metal-Mediated and Metal-Catalyzed Reactions of Isocyanides. *Chem. Rev.* **2015**, *115*, 2698–2779.
- (33) Ruiz, J.; Sol, D.; Mateo, M. A.; Vivanco, M. Selective formation of formamidines, carbodiimides and formimidates from isocyanide complexes of Mn(I) mediated by Ag₂O. *Dalton Trans.* **2018**, *47*, 6279–6282.
- (34) Chikamori, H.; Takao, T. Formation of a μ 3 - Acetylide on a Ru₃ Cluster via Coupling of μ -Methylene with Isocyanide Accompanied by Elimination of Amine: A Model of Hydrogen-Assisted C – C Bond Formation on a Metal Surface. *Organometallics* **2019**, *38*, 2705–2709.
- (35) Collet, J. W.; Roose, T. R.; Ruijter, E.; Maes, B. U. W.; Orru, R. V. A. Base Metal Catalyzed Isocyanide Insertions. *Angew. Chem., Int. Ed.* **2020**, *59*, 540–558.
- (36) Luo, J.; Chen, G.-S.; Chen, S.-J.; Li, Z.-D.; Liu, Y.-L. Catalytic Enantioselective Isocyanide-Based Reactions: Beyond Passerini and Ugi Multicomponent Reactions. *Chem. - Eur. J.* **2021**, *27*, 6598–6619.
- (37) Albano, V. G.; Busetto, L.; Marchetti, F.; Monari, M.; Zacchini, S.; Zanotti, V. Alkyne - Isocyanide Coupling in $[\text{Fe}_2(\text{CNMe})(\text{CO})_3(\text{Cp})_2]$: A New Route to Diiron μ -Vinyliminium Complexes. *Organometallics* **2007**, *26*, 3448–3455.
- (38) Schoch, S.; Braccini, S.; Biancalana, L.; Pratesi, A.; Funaioli, T.; Zacchini, S.; Pampaloni, G.; Chiellini, F.; Marchetti, F. When Ferrocene and Diiron Organometallics Meet: Triiron Vinyliminium Complexes Exhibit Strong Cytotoxicity and Cancer Cell Selectivity. *Inorg. Chem. Front.* **2022**, *9*, 5118–5139.
- (39) Since the ferrocenyl unit is not connected to the Fe-Fe core and thus not directly involved in cooperativity mechanisms, the triiron compound **1** is viewed in this text as a ferrocenyl-decorated diiron complex.
- (40) Knorr, M.; Jourdain, I.; Lentz, D.; Willemsen, S.; Strohmman, C. Synthesis and reactivity of dinuclear iron-platinum, chromium-platinum, molybdenum-platinum and tungsten-platinum complexes with bridging carbonyl, isocyanide and aminocarbene ligands. An empirical study on the parameters decisive for the bonding mode of the isocyanide ligand. *J. Organomet. Chem.* **2003**, *684*, 216–229.
- (41) Biancalana, L.; Ciancaleoni, G.; Zacchini, S.; Pampaloni, G.; Marchetti, F. Carbonyl-isocyanide mono-substitution in $[\text{Fe}_2\text{Cp}_2(\text{CO})_4]$: A re-visitation. *Inorg. Chim. Acta* **2020**, *517*, No. 120181.
- (42) Ennis, M.; Kumar, R.; Manning, A. R.; Howell, J.A.S.; Mathur, P.; Rowan, A. J.; Stephens, F. S. Spectroscopic study of the structures of $[\text{M}_2(\eta\text{-C}_3\text{H}_5)_2(\text{CO})_n(\text{CNR})_{4-n}]$ complexes ($n = 1$ or 2 ; $\text{M} = \text{Fe}$ or Ru) in solution. The structure of $\text{cis}[(\eta\text{-C}_3\text{H}_5)(\text{OC})\text{Fe}(\mu\text{-CO})(\mu\text{-CNP}^r)\text{Fe}(\text{CNP}^r)(\eta\text{-C}_3\text{H}_5)]$ in the solid state. *J. Chem. Soc., Dalton Trans.* **1981**, 1251–1259.
- (43) Marchetti, F. Alkylidyne and Alkylidene Complexes of Iron. In *Comprehensive Organometallic Chemistry IV*; Parkin, G.; Meyer, K.; O'Hare, D., Eds.; Elsevier: Kidlington, UK, 2022; Vol. 7, pp 210–257.
- (44) Bresciani, G.; Boni, S.; Zacchini, S.; Pampaloni, G.; Bortoluzzi, M.; Marchetti, F. Alkyne – alkenyl coupling at a diruthenium Complex. *Dalton Trans.* **2022**, *51*, 15703–15715.
- (45) Casey, C. P.; Vosejka, P. C. Addition of Carbon Nucleophiles to (π -Alkenyl)diiron Complexes. *Organometallics* **1988**, *7*, 934–936.
- (46) Hoffbauer, M. R.; Iluc, V. M. [2+2] Cycloadditions with an Iron Carbene: A Critical Step in Enyne Metathesis. *J. Am. Chem. Soc.* **2021**, *143*, 5592–5597.
- (47) Chakarawet, K.; Davis-Gilbert, Z. W.; Harstad, S. R.; Young, V. G., Jr.; Long, J. R.; Ellis, J. E. Ta(CNDipp)₆: An Isocyanide Analogue of Hexacarbonyltantalum(0). *Angew. Chem., Int. Ed.* **2017**, *56*, 10577–10581.
- (48) Yamamoto, Y. Zerovalent Transition Metal Complexes of Organic Isocyanides. *Coord. Chem. Rev.* **1980**, *32*, 193–233.
- (49) Busetto, L.; Marchetti, F.; Zacchini, S.; Zanotti, V. Addition of Isocyanides at Diiron μ -Vinyliminium Complexes: Synthesis of Novel Ketenimine - Bis(alkylidene) Complexes. *Organometallics* **2008**, *27*, 5058–5066.
- (50) Biancalana, L.; Fiaschi, M.; Ciancaleoni, G.; Pampaloni, G.; Zanotti, V.; Zacchini, S.; Marchetti, F. A comparative structural and spectroscopic study of diiron and diruthenium isocyanide and aminocarbene complexes. *Inorg. Chim. Acta* **2022**, *536*, No. 120886.
- (51) Guillevic, M. A.; Hancox, E. L.; Mann, B. E.; Reinvestigation, A. of the Solution Structure and Dynamics of $[\text{Fe}_2\text{Cp}_2(\text{CO})_{4-n}(\text{CNMe})_n]$, $n = 1$ or 2 . *J. Chem. Soc. Dalton Trans.* **1992**, 1729–1733.
- (52) Fehlhammer, W. P.; Schroder, A.; Sperber, W.; Fuchs, J. Diisenkomplexe mit Acylisocyanid- und Iminoacyl-isocyanid-Briick-enliganden. *Chem. Ber.* **1992**, *125*, 1087–1092.
- (53) Knorr, M.; Jourdain, I.; Mohamed, A. S.; Khatyr, A.; Koller, S. G.; Strohmman, C. Synthesis and reactivity of bis-

(diphenylphosphino)amine-bridged heterobimetallic iron-platinum m-isonitrile and m-aminocarbyne complexes. *J. Organomet. Chem.* **2015**, *780*, 70–85.

(54) Marchetti, F.; Zacchini, S.; Zanotti, V. Coupling of Isocyanide and μ -Aminocarbyne Ligands in Diiron Complexes Promoted by Hydride Addition. *Organometallics* **2014**, *33*, 3990–3997.

(55) Marchetti, F.; Zacchini, S.; Zanotti, V. C – N Coupling of Isocyanide Ligands Promoted by Acetylide Addition to Diiron Aminocarbyne Complexes. *Organometallics* **2015**, *34*, 3658–3664.

(56) Albano, V. G.; Busetto, L.; Marchetti, F.; Monari, M.; Zacchini, S.; Zanotti, V. Hydride addition at μ -vinyliminium ligand obtained from disubstituted alkynes. *J. Organomet. Chem.* **2005**, *690*, 837–846.

(57) Knorr, M.; Faure, T.; Braunstein, P. Synthesis of the heterodinuclear Fe-Pt complex $[(OC)_3Fe\{\mu-CN(2,6\text{-xylyl})\}(\mu\text{-dppm})PtPPh_3]$ containing a bridging isonitrile ligand and electrophilic additions leading to μ -aminocarbyne complexes. *J. Organomet. Chem.* **1993**, *447*, C4–C6.

(58) Pombeiro, A. J. L.; Guedes da Silva, M. F. C.; Michelin, R. A. Aminocarbyne complexes derived from isocyanides activated towards electrophilic addition. *Coord. Chem. Rev.* **2001**, *218*, 43–74.

(59) Knorr, M.; Strohmann, C. Syntheses, Structures, and Reactivity of Dinuclear Molybdenum–Platinum and Tungsten–Platinum Complexes with Bridging Carbonyl, Sulfur Dioxide, Isonitrile, and Aminocarbyne Ligands and a dppa Backbone (dppa = $Ph_2PNHPPPh_2$). *Organometallics* **1999**, *18*, 248–257.

(60) DeLaet, D. L.; Fanwlck, P. E.; Kubiak, C. P. Binuclear Complexes of Nickel(0): Comparison of a Bridging Methyl Isocyanide and a Bridging (Methylamino)carbyne Ligand. *Organometallics* **1986**, *5*, 1807–1811.

(61) Grundy, K. R.; Robertson, K. N. Binuclear Isocyanide Complexes of Platinum(I). Facile N-Protonation and Alkylation of Bridging Isocyanide Ligands To Yield Bridging Aminocarbyne Complexes. *Organometallics* **1983**, *2*, 1736–1742.

(62) Albano, V. G.; Busetto, L.; Carlucci, L.; Cristina Cassani, M.; Monari, M.; Zanotti, V. Synthesis of dinuclear iron and ruthenium aminoalkylidene complexes and the molecular structure of the novel *cis*- $[Ru_2(CO)_2(Cp)_2\{\mu-C(CN)N(Me)Bz\}_2]$ ($Cp = \eta\text{-C}_5\text{H}_5$; $Bz = CH_2Ph$). *J. Organomet. Chem.* **1995**, *488*, 133–139.

(63) Cox, G.; Dowling, C.; Manning, A. R.; McArdle, P.; Cunningham, D. A reinvestigation of the reaction of $[Fe_2(\eta\text{-C}_5\text{H}_5)_2(CO)_{4+n}(CNR)_n]$ ($n = 1$ or 2) with strong alkylating agents. *J. Organomet. Chem.* **1992**, *438*, 143–158.

(64) Dowling, C.; Manning, A. R. The reaction of $[Fe_2(\eta\text{-C}_5\text{H}_5)_2(CO)(CNMe)(\mu\text{-CO})(\mu\text{-CNMe}_2)]^+$ salts with trifluoromethanesulphonic acid ($HOSO_2CF_3$). *J. Organomet. Chem.* **1996**, *507*, 281–282.

(65) A green solid was obtained after filtration of the reaction mixture through celite, which was washed with diethyl ether, dried under vacuum and analysed. IR (CH_2Cl_2): $\tilde{\nu}/cm^{-1} = 2195w$ (C_6N), $2012s$ (CO), $1745m$ (OCO) $1562m$ ($\mu\text{-CN}$). 1H NMR (acetone- d_6): $\delta/ppm = 6.11$ (s, 1 H, $C\beta H$); 5.57 , 5.47 , 5.29 , 5.14 (s, 10 H, Cp); 4.49 , 4.47 (s, 5 H, CpFc); 4.47 , 4.05 (s, 3 H, NMe); 2.56 , 2.54 (s, 6 H, NMe $_2$); 1.42 , 1.33 (t, 6 H, CH_2CH_3). $^{13}C\{^1H\}$ NMR (CD_3OD): $\delta/ppm = 94.5$, 94.3 , 89.2 , 89.0 , (Cp); 71.1 , 71.0 (CpFc); 74.6 , 70.2 , 69.8 , 68.1 , 67.5 (CSH_4); 14.5 (OCH_2CH_3). Isomer ratio = 5:3.

(66) Bresciani, G.; Biancalana, L.; Pampaloni, G.; Zacchini, S.; Ciancaleoni, G.; Marchetti, F.; Comprehensive, A. Analysis of the Metal–Nitrile Bonding in an Organo-Diiron System. *Molecules* **2021**, *26*, 7088.

(67) Pombeiro, A. J. L. Electron-donor/acceptor properties of carbynes, carbenes, vinylidenes, allenylidenes and alkynyls as measured by electrochemical ligand parameters. *J. Organomet. Chem.* **2005**, *690*, 6021–6040.

(68) Venâncio, A. I. F.; Guedes da Silva, M. F. C.; Martins, L. M. D. R. S.; Fraústo da Silva, J. J. R.; Pombeiro, A. J. L. Allenylidene Iron(II) Complexes and Their Deprotonation, Nucleophilic Addition Reactions, and Cathodic Protonation toward Alkynyl Derivatives: A

Chemical and Electrochemical Study. *Organometallics* **2005**, *24*, 4654–4665.

(69) Fromm, S. F. T.; Green, M.; Mercer, R. J.; Nagle, K. R.; Orpen, A. G.; Schwiegk, S. Evidence for a facile switch in the bonding mode of μ -vinylidene ligands from σ, η^2 to σ, σ ; synthesis and structure of a dinuclear $\mu\text{-}\sigma, \eta^2$ -allenylidene complex. *J. Chem. Soc., Chem. Commun.* **1986**, 1666–1668.

(70) Edwards, A. J.; Esteruelas, M. A.; Lahoz, F. J.; Modrego, J.; Oro, L. A.; Schrickel, J. Synthesis, Structure, and Bonding of the Unusual $\mu\text{-}\sigma, \sigma$ -Allenylidene Complex $[Rh_2(\mu\text{-OOCCH}_3)(\mu\text{-}\sigma, \sigma\text{-CCCPh}_2)(CO)_2(PCy_3)_2]BF_4$. *Organometallics* **1996**, *15*, 3556–3562.

(71) Bresciani, G.; Biancalana, L.; Zacchini, S.; Pampaloni, G.; Ciancaleoni, G.; Marchetti, F. Diiron bis-cyclopentadienyl complexes as transfer hydrogenation catalysts: The key role of the bridging aminocarbyne ligand. *Appl. Organomet. Chem.* **2022**, *37*, No. e6990.

(72) Tsurugi, H.; Laskar, P.; Yamamoto, K.; Mashima, K. Bonding and structural features of metal-metal bonded homo- and heterodinuclear complexes supported by unsaturated hydrocarbon ligands. *J. Organomet. Chem.* **2018**, *869*, 251–263.

(73) Menges, F. Spectragryph - optical spectroscopy software", Version 1.2.5, @ 2016-2017. <http://www.ffmpeg2.de/spectragryph>.

(74) Fulmer, G. R.; Miller, A. J. M.; Sherden, N. H.; Gottlieb, H. E.; Nudelman, A.; Stoltz, B. M.; Bercaw, J. E.; Goldberg, K. I. NMR Chemical Shifts of Trace Impurities: Common Laboratory Solvents, Organics, and Gases in Deuterated Solvents Relevant to the Organometallic Chemist. *Organometallics* **2010**, *29*, 2176–2179.

(75) Willker, W.; Leibfritz, D.; Kerssebaum, R.; Bermel, W. Gradient selection in inverse heteronuclear correlation spectroscopy. *Magn. Reson. Chem.* **1993**, *31*, 287–292.

(76) The 31P NMR spectrum of uncoordinated diethyl isocyanomethylphosphonate, in $CDCl_3$ solution, displays a resonance at 14.0 ppm.

(77) Sheldrick, G. M. Crystal structure refinement with SHELXL. *Acta Crystallogr., Sect. C: Struct. Chem.* **2015**, *71*, 3–8.

(78) Becke, A. D. Density-functional thermochemistry. V. Systematic optimization of exchange-correlation functionals. *J. Chem. Phys.* **1997**, *107*, 8554.

(79) Weigend, F. Accurate Coulomb-fitting basis sets for H to Rn. *Phys. Chem. Chem. Phys.* **2006**, *8*, 1057–1065.

(80) Grimme, S. Semiempirical GGA-type density functional constructed with a long-range dispersion correction. *J. Comput. Chem.* **2006**, *27*, 1787–1789.

(81) Glendening, E. D.; Badenhop, J. K.; Reed, A. E.; Carpenter, J. E.; Bohmann, J. A.; Morales, C. M.; Karafiloglou, P.; Landis, C. R.; Weinhold, F. *NBO 7.0*; Theoretical Chemistry Institute, University of Wisconsin: Madison, WI, 2018.